

Design of the Lower Control Arm of an Electric SUV Front Suspension Based on Multi-Disciplinary Optimization Technology

Zhenqi Yu^{1,2}, Huifang Jia², and Xingyuan Huang^{3*}

¹Nanchang Institute of Technology, Nanchang 330044, China

²Product Development & Technical Center, Jiangling Motors Co., Ltd, Nanchang 330001, China

³School of Mechatronics Engineering, Nanchang University, Nanchang 330031, China

Received July 18 2020

Accepted Feb 20 2021

Abstract

An electric SUV is designed and developed based on the original traditional fuel vehicle model. The design scheme of the front suspension lower control arm of prototype vehicle is referred to save the development cycle and cost of the design. The original design scheme is optimized to meet the performance and lightweight requirements. In this paper, the analysis model of lower control arm is firstly established based on the finite element technology to conduct free modal analysis. The results show that the first two modes appear as bending and torsion. The modal frequency is higher than excitation frequency, which satisfies the requirement of vibration characteristics. Then free modal test on lower control arm is carried out based on hammer method, and the test results show that the accuracy of the analysis value is high. Then, the front suspension dynamics model of electric SUV model is established to extract the load of lower control arm. The inertial release method is applied to analyze its limit strength, the results show that its maximum stress is lower than its used stress which meets the requirements of strength design. Finally, the multidisciplinary optimal design of lower control arm is carried out to obtain the best design scheme. After optimization, both modal characteristics and strength characteristics meet the design requirements, and its mass is reduced by 16.7%. And its optimization scheme has passed the bench test and road test certificate successfully, so it has high accuracy and feasibility, providing a new idea for the design and development of the lower control arm, the front suspension of electric SUV.

© 2021 Jordan Journal of Mechanical and Industrial Engineering. All rights reserved

Keywords: lower control arm; modal; inertia release; strength; optimization; bench test;

1. Introduction

The suspension structure of electric vehicle is an important system which guarantees the stability and comfort of the vehicle. As the guiding and force transmission component of the former Macphersan suspension, lower control arm is connected with the wheels and subframes by ball hinges and bushings to withstand forces and torques from both vertical and horizontal directions when the vehicle is moving, which may make abnormal noise and failure risk occur. Its vibration characteristics and strength characteristics directly affect the safety and reliability of the vehicle, while lightweight affects the endurance mileage and manufacturing cost of the vehicle. Therefore, the design of lower control arm needs to consider various performance requirements and lightweight requirements. In order to save development cycle and cost, the optimization is carried out according to the front suspension lower control arm of original traditional fuel SUV models, which makes the structure of lower control arm meet the performance requirements required by electric SUV.

Fuchs Hannes et al. ^[1] discuss the results of a study to develop lightweight steel proof-of-concept front lower control arm (FLCA) designs that are less expensive and achieve equivalent structural performance relative to a baseline forged aluminum FLCA assembly. Yoo, Sang Hyuk et al. ^[2] show topology optimization of lower control arm (LCA), made of carbon fiber reinforced plastic (CFRP), that was originally composed of aluminum alloy, and authors propose the new design of CFRP LCA with 30% weight reduction compared to Al alloy LCA. Heo, S.J. et al. ^[3] presents shape optimization of lower control arm considering multi-disciplinary (stiffness, strength and durability) constraint conditions, and the optimal model meets all the design constraint conditions and reduces the weight by about 200 grams comparing with that of the initial model. Huang He ^[4] conducts stiffness performance analysis, strength performance analysis and modal performance analysis on a certain lower control arm and optimizes its structure and obtained its lightweight scheme. Its weight is significantly reduced after optimization, which also meets the requirements of fatigue life.

The following is the method to analyze whether the static and dynamic performance of the front suspension lower

* Corresponding author e-mail: huangxingyuan001@126.com.

control arm of an electric SUV can meet the design requirements. Firstly, the free modal analysis is carried out based on finite element method; secondly, the modal test is carried out to verify the accuracy of the model; thirdly, the dynamic simulation analysis of the front suspension is carried out to obtain the load of its typical working condition, and then the strength analysis is carried out; fourthly, the lightweight design is carried out on the basis of multiple disciplines and multiple objectives; finally, bench test and road test are carried out.

2. Dynamic characteristics analysis of lower control arm

2.1. Build finite element model

This type of electric SUV front suspension lower control arm follows the design scheme of the prototype fuel car. It is mainly composed of upper plate, lower plate and reinforcing shaft tube, its front point and back point are connected with the sub-frame, and its external point is connected with the steering knuckle. The 3d model of lower control arm is established using Catia software and imported into Hypermesh software^[5,6]. The middle surface of upper plate, lower plate and reinforced shaft tube is extracted, and processed by grid division using 4mm mixed unit (CTRIA3 unit and CQUAD4 unit). It should be ensured that it is quadrilateral elements, and triangular elements should be reduced. Weld joint between each other is replaced by aligned quadrilateral shell elements. The thickness of upper plate of lower control arm is 4.0 mm, the thickness of lower plate is 4.0 mm, the thickness of reinforced shaft tube is 4.5 mm, and the mass of lower control arm is 4.2 kg. The material of each part of lower control arm is QSTE420TM, its yield strength is 420 MPa, the tensile strength is 480 MPa, the fracture strain is 21%. The material properties are shown in Table 1. The materials and their attributes of the same property are established to create a lower control arm finite element model, as shown in Fig. 1.

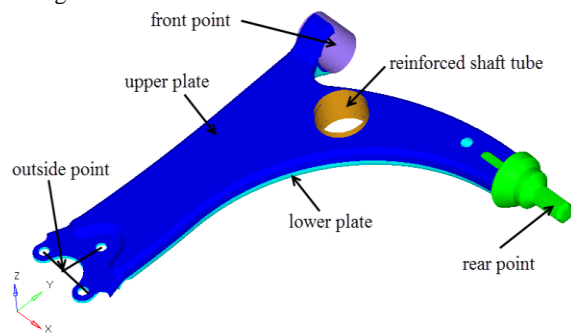


Figure 1. Finite element model of lower control arm

Table 1. material properties of QSTE420TM

Name	Elastic Modulus	Poisson's ratio	Density
QSTE420TM	210GPa	0.3	7.9E3 kg/m ³

2.2. Analysis of modal results

Based on general theory of modal analysis as well-known^[7,8], free modal analysis is conducted on the lower control arm using Nastran software^[9,10] to obtain the result

that the first two natural frequencies are 610.8 Hz and 693.5 Hz, and their mode shapes are shown as bending and torsion respectively. What is shown in Fig. 2 and Fig. 3 are the torsional and bending modal shapes of the front suspension lower control arm respectively. The excitation frequency of the tire cavity was 180.5 Hz, and the excitation frequencies range of the motor were 16.7 Hz-200 Hz. Through modal analysis, it can be known that the lower control arm belongs to high-order frequency structure, which is far higher than the excitation frequency of its motor and the frequency of tire cavity, so it can meet the requirements of modal characteristics.

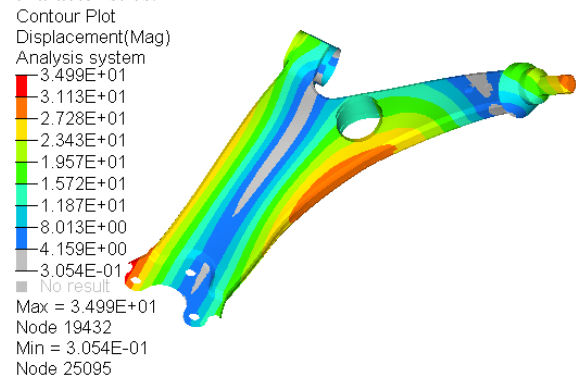


Figure 2. Bending modal shape of lower control arm

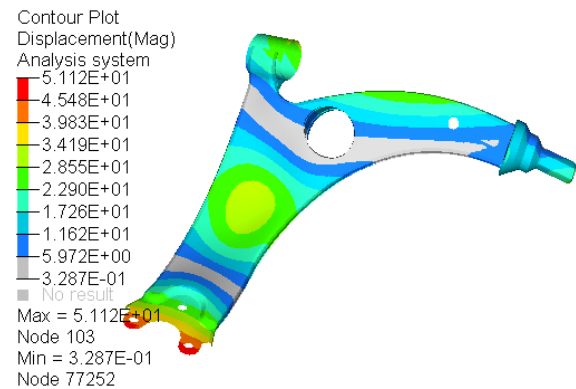


Figure 3. torsional modal shape of lower control arm

3. Modal test of lower control arm

In order to verify the accuracy of modal analysis of lower control arm, elastic rope is adopted to suspend the lower control arm on the platform, and free-modal tests are conducted on the basis of hammer method^[11,12] and LMS Test.Lab platform, The experimental equipment includes LMSTest.Lab13.0 test software, LMS data collector, DELL laptop, 4 pcs of 356A16 modal vibration sensor from PCB company, ICP hammer, network cable and BNC cable, as shown in Fig. 4.

Since the lower control arm free-modal test needs to be placed in a free state, an elastic rubber cable is used to suspend the lower control arm in the test to make it in a balanced and free state. Six acceleration sensors are arranged on the arm, which should be placed as far as possible in obvious vibration. The channel of the hammer input is defined as the reference channel using the LMS Test.Lab test software. The direction of the excitation point should be consistent with the reference direction. Multi-point input free modal test method for multi-point output response of excitation. Try to keep the magnitude of the

excitation force consistent during each excitation during the experiment. Each measurement point is unidirectionally excited five times. At the same time, the relationship between the excitation and response is checked to ensure that the coherence coefficient is close to 1. To ensure that the stimulus signal is valid. The excitation signal measured by the acceleration sensor is converted into a frequency response function by using LMS Test.Lab software. The resulting frequency response graph is shown in Figure 5.

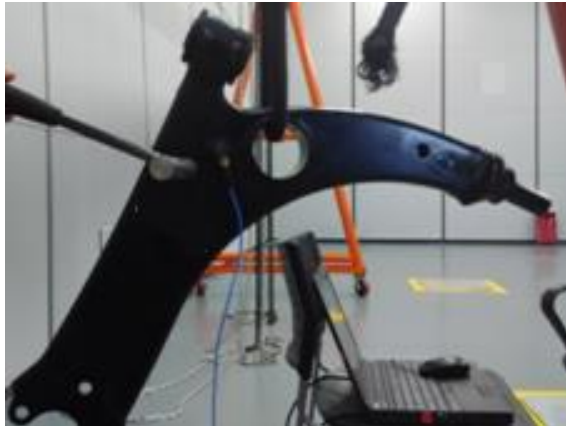


Figure 4. Modal test of lower control arm

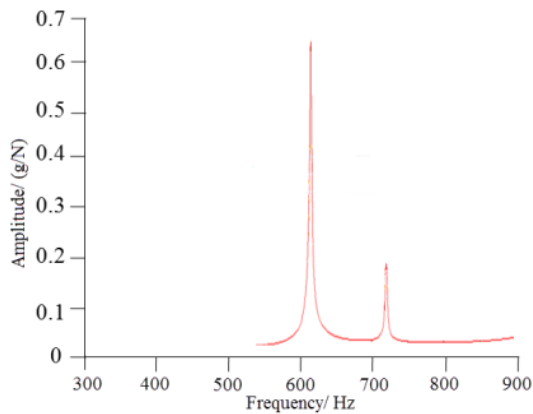


Figure 5. Frequency response graph

The modal shapes of the lower control arm obtained through experiments are shown in Figures 6 and 7. The modal shapes are consistent with those of the previous analysis.

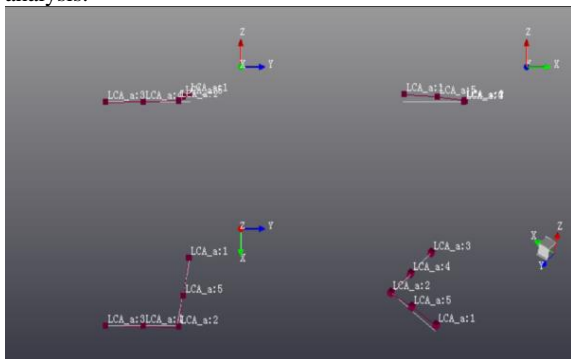


Figure 6. Bending modal shape of lower control arm

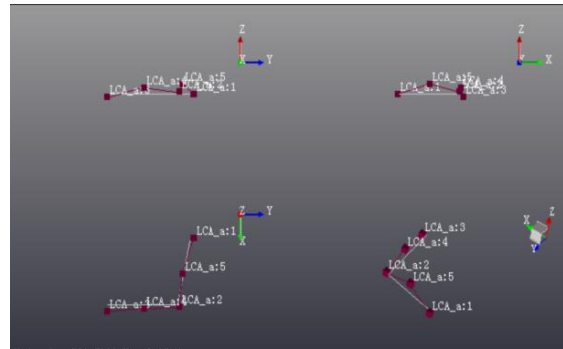


Figure 7. torsional modal shape of lower control arm

What is shown in Table 2 is comparison of analysis value and test value of lower control arm modal frequency. As shown in Table 1, the analysis value of the lower control arm's modal frequency is basically the same as the test value, and the relative errors of the first two orders are 1.5% and 3.3% respectively, which proves the accuracy of finite element modeling and analysis.

Table 2. lower control arm modal frequency comparison

	Test value/Hz	Analysis value/Hz	Relative error
First-order modal frequency	620.3	610.8	1.5%
Second-order modal frequency	717.2	693.5	3.3%

4. Static strength analysis of lower control arm

4.1. Force analysis of typical working conditions

The typical working conditions of vehicles in the process of driving are divided into brake vertical impact and turning. The stress states of tyre junction under each working condition are calculated according to vehicle parameters. The relevant vehicle parameters of this electric vehicle are shown in Table 3 with obvious changes compared with the raw fuel vehicle. The structural optimization of the front suspension lower control arm should be carried out according to the whole vehicle parameters of electric vehicle.

Table 3. Vehicle Parameters

Parameter	Value
Mass on front axle	850 kg
Mass on rear axle	950 kg
Height of center of gravity	0.65 m
Axle distance	2.6 m
Wheelbase	1.6 m

The braking conditions is taken as an example:

$$F_z = \frac{1}{2} M_F \times g + (M_F + M_R) \times a \times \frac{H}{2L} \quad (1)$$

$$F_x = F_z \times \mu \quad (2)$$

where: F_z is the vertical load on the tire junction of this type of electric SUV; F_{x1} is the longitudinal load on the tire landing place of this type of electric SUV; M_F is mass

on the front axle; M_R is mass on the rear axle; g is the acceleration of gravity; H is the center of gravity height of ; L is the wheelbase ; a_1 is the braking acceleration of type, which is 1.0 g; μ is ground adhesion coefficient, which is 1.0 [13-15]. The stress at the tire junction can be obtained by the above vehicle parameters and the corresponding calculation formula, and the stress state at the tire junction in other working conditions can be obtained by analogy.

4.2. Dynamic simulation analysis of front suspension

The front suspension model is established based on the coordinate information, vehicle parameters and performance curve of the connection points of the electric vehicle front suspension system by using Adams/Car Platform [16], which is as shown in Fig. 8. The force states of the tire ground points under the above operating conditions are input into its front suspension model, so that dynamic simulation analysis can be performed to extract the load at the front and rear points and the outside points of the lower control arm respectively under braking vertical impact and turning conditions.

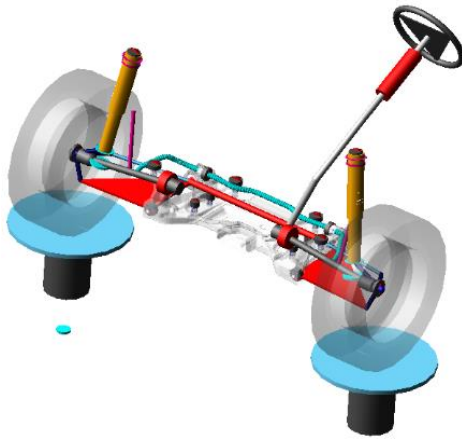


Figure 8. Adams/Car model of front suspension

4.3. Strength result analysis

Based on Nastran software and using the inertial release method [17] to load the loads extracted from the multi-body dynamics model, as shown in Table 4. The forces in the table are the forces that the connector reacts on the lower control arm. The inertia release method is based on loading inertial force to balance the external load, make it balance, and then solve the stress distribution. The force balance equation of the inertial release method can be expressed as:

$$\{F\} + M\{\ddot{\sigma}\} = 0 \quad (3)$$

$\{F\}$ is the external load matrix of the finite element

node, $\{\ddot{\sigma}\}$ is the acceleration matrix of the finite element node, and M is the mass matrix. By solving equation (3), the node acceleration and inertial force required to maintain balance at each node can be obtained, and then the inertial force of the node is loaded on the node as an external load, thereby constructing a self-balancing force system. Since the external load is balanced by the acceleration load of each node, the restraining force of the restraint point is zero, which can reduce the influence of restraint points on the stress results, improve the calculation accuracy, and obtain more reasonable stress results. If the inertial load is regarded as an external load, then the system will have the same external load and the inertial load under the constant acceleration state, that is, the static equilibrium state will be reached.

the ultimate strength analysis was performed without any constraints. The strength analysis of the electric vehicle lower control arm is carried out to obtain its stress distribution under various working conditions. The inertial release method refers to solving the acceleration required by each node in order to maintain balance, and then obtaining the inertial force of each node, and then loading the inertial force of the node as an external force on the node of the finite element, then a self-balanced force system can be constructed. That is, the inertia force of the structure is used to balance with the external force.

Table 4. Loads extracted from the multi-body dynamics model

	X (N)			Y (N)			Z (N)		
	braking	impact	turning	braking	impact	turning	braking	impact	turning
Outside point	9317	-1938	266	-1840	-5000	-1124	306	-109	-54
Front point	-7573	1653	-219	12888	2762	1442	169	46	93
Rear point	-1744	285	47	-11048	2238	-318	-465	63	-39

What is shown in Fig. 9, Von Mises Equivalent stress contour plot of lower control arm braking condition. According to Fig. 9, the maximum stress of lower control arm during braking is 301.2 MPa, which is located at the front bend of lower control arm. This is because the whole axle load of the vehicle transfers to the front-end during braking, resulting in relatively large longitudinal stress. What is shown in Fig. 10, is the Von Mises Equivalent stress contour plot of lower control arm under the vertical impact condition. According to Fig. 10, the maximum stress value of the lower control arm during vertical impact is 98.7 MPa, which is located near the connection between the outer point of the lower control arm and the steering knuckle. Because the phenomenon of stress concentration at the outer point of the vehicle due to the vertical impact force acting vertically downward. As shown in Fig. 11, is the Von Mises Equivalent stress contour plot under lower control arm's turning condition. It can be known from Fig. 11 that the maximum stress value of lower control arm during turning is 31.9 MPa. In practical engineering, the safety factor of the component is generally 1.2, and the yield strength of lower control arm material is 420 MPa. Allowable stress as the maximum stress value that the structure can withstand is equal to the yield strength of the material divided by the safety factor. that is the allowable stress is 350 MPa. Therefore, the maximum stress of the lower control arm under three typical working conditions is lower than its allowable stress, which conforms to the design requirements of ultimate strength characteristics.

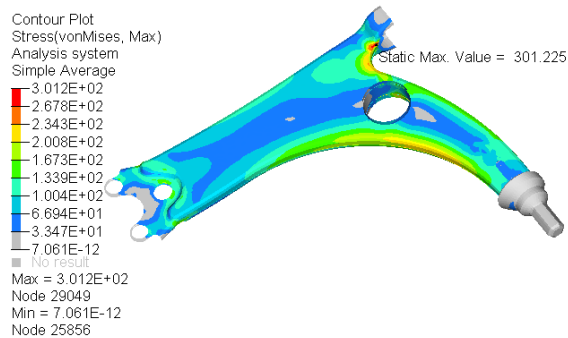


Figure 9. Von Mises Equivalent stress contour plot of lower control arm (braking condition)

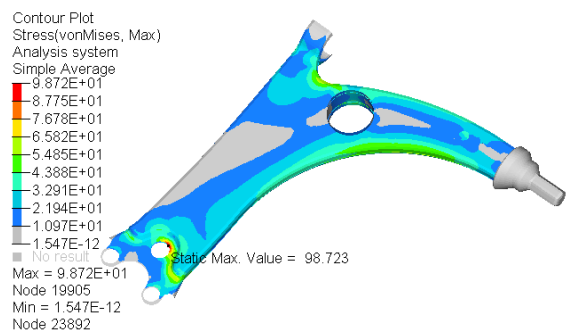


Figure 10. Von Mises Equivalent stress contour plot of lower control arm (vertical impact condition)

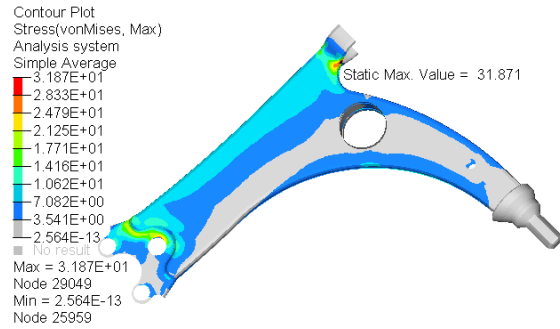


Figure 11. Von Mises Equivalent stress contour plot of lower control arm (turning condition)

5. Multi-disciplinary optimization analysis

5.1. Establishment of optimization model

In order to carry out lightweight design on the lower control arm and ensure its modal characteristics and strength performance, the thickness values of the upper and lower board and strengthened shaft tube of the lower control arm are taken as design variables, and the minimum mass of the lower control arm is taken as the target response function. Due to lower stress level of lower control arm in the vertical impact condition and turning condition, in order to improve optimization efficiency, that only the maximum stress under braking condition is lower than the allowable stress (350 MPa) and the first-order natural frequency is not lower than 95% (580.3 Hz) of the initial frequency is taken as constraint conditions to establish the optimization model. Minimize Weight (a,b,c)

$$\text{Subject to } \begin{cases} \text{Weight} < 4.2 \\ \text{Stress} < 350 \\ \text{Modal} > 580.3 \end{cases} \quad (3)$$

where: *Weight* is total mass of lower control arm; *Stress* is the maximum stress of lower control arm under braking condition; *Modal* is the first inherent frequency of lower control arm; *a* is the thickness of lower control arm upper plate; *b* is the thickness of lower control arm lower plate; *c* is the thickness of strengthen shaft tube of lower control arm;

5.2. Optimization results analysis

Its finite element model, modal analysis, and strength analysis are integrated based on the optimization mathematical model and the Isight platform [18], as shown in Fig. 12. The lower control arm finite element model source file are imported into the HyperMesh assembly, the upper plate thickness, the lower plate thickness and the reinforced shaft tube thickness are processed by the input parameters analysis (parametric processing), and set as the design variable; its static strength analysis source file and its result file are imported into the Strength component, and the maximum stress in braking conditions is processed by output parameter analysis; its modal analysis source file and its result file are imported into the Mode component to analyze the output parameters of its first-order frequency; the neighborhood cultivation genetic algorithm, regards each target as equally important. The method of adjacent

breeding is achieved by sorting and grouping to cross, so that the probability of cross breeding of solutions close to the Pareto front is increased, and the calculation convergence process is accelerated. Improved efficiency is selected in the optimization component, and the target response function and design variable range are set to perform multidisciplinary optimization analysis of lower control arm. What is shown in Fig. 13 is the optimal iteration curve for the mass of lower control arm. After 99 iterations of Iisght platform, the optimal design variables of lower control arm are finally obtained. Table 5 shows the comparison of parameters before and after optimization. According to Table 4, after optimization, the upper board thickness of lower control arm is 3.6 mm, the lower board thickness of lower control arm is 3.2 mm, and the strengthened shaft tube thickness of lower control arm is 3.5 mm.

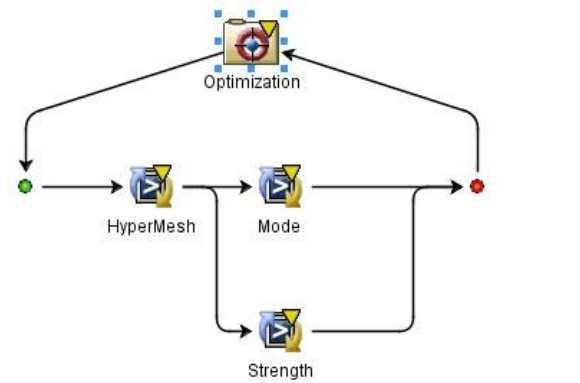


Figure 12. Iisght platform

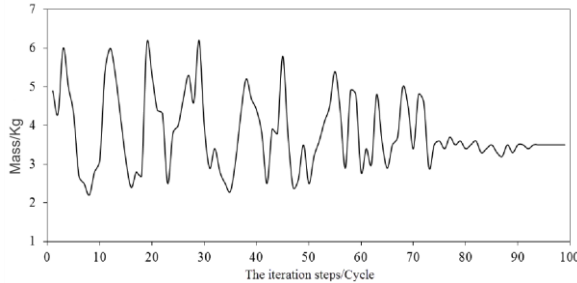


Figure 13. Mass optimization iteration curve of lower control arm

Table 5. Comparison of Parameters before and after Optimization

Parameters	Before optimization	After optimization
Upper plate thickness/mm	4.0	3.6
Lower plate thickness/mm	4.0	3.2
Reinforced shaft tube thickness/mm	4.5	3.5
Lower arm weight/kg	4.2	3.5
Maximum stress in braking conditions/MPa	301.2	346.4
Maximum stress in vertical impact conditions/MPa	98.7	163.2
Maximum stress in turning conditions /MPa	62.5	135.3
First-order frequency/Hz	610.8	585.7
Second-order frequency/Hz	693.5	661.2

Based on the optimal design variables, modal check analysis and strength check analysis are carried out on lower control arm. As shown in Table 3, the first two modal frequencies of lower control arm after optimization are 585.7 Hz and 661.2 Hz, both of which are higher than 95% of the initial frequency. Their modal performances are approximately the same, and all meet the requirements of modal characteristics. The reduction of the thickness of the lower control arm plate will lead to a reduction in its stiffness, but to a certain extent, it has a small impact on the dynamic performance of the suspension.

What is shown in Fig. 14 is the stress distribution cloud diagram which lower control arm’s braking condition after optimization is used. As can be seen from Fig. 12, after optimization, the maximum stress of lower control arm in braking is 346.4 MPa and lower than its permitted stress, which meets the strength design requirements. As can be seen from Table 4, the maximum stress of lower control arm under vertical impact and turning conditions is 163.2 MPa and 135.3 MPa respectively, and its strength safety coefficient is 2.6 and 3.1 respectively, both are lower than its allowable stress. After optimization, the mass of lower control arm is reduced to 3.5 kg, and 16.7% of the mass is successfully reduced, with relatively obvious overall optimization effect.

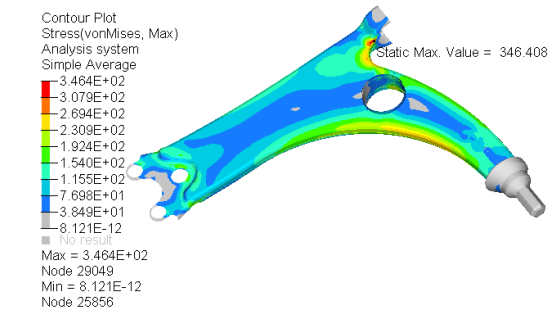


Figure 14. Von Mises Equivalent stress contour plot of lower control arm optimization scheme (braking condition)

6. Test and Analysis

In order to verify and check the feasibility and accuracy of the lower control arm optimization scheme, the bench test platform of lower control arm is built, as shown in Fig. 13. The lower control arm is under the most stress during braking conditions. In order to verify the strength performance of the arm optimization scheme, the front and rear points of the arm are fixed, and a longitudinal load of 9,500 N is applied to its outer point (based on the Adams model to extract the brake condition load), the schematic representation as shown in Fig. 14. After the test completed, the lower control arm does not crack and deform, so its strength analysis has high reliability.

And tested for durability is necessary, the outer point and the front point of lower control arm are fixed, longitudinal force of 3,000 N in a sinusoidal manner is applied on the latter point with a frequency of 1 Hz, the schematic representation as shown in Fig. 15. And no cracking is found after the test is conducted for 300,000 cycles. Referring to Figure 15, a similar approach is taken to fix the front and rear points of lower control arm, and longitudinal force of 15,000 N in a sinusoidal manner is applied on its

external points with a frequency of 1 Hz, And no cracking is found after the test is conducted for 300,000 cycles.

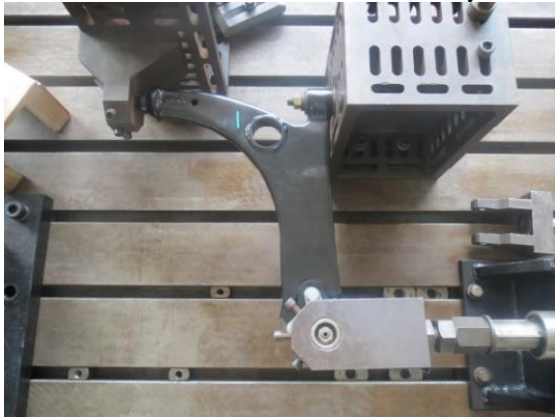


Figure 13. The bench test platform of lower control arm

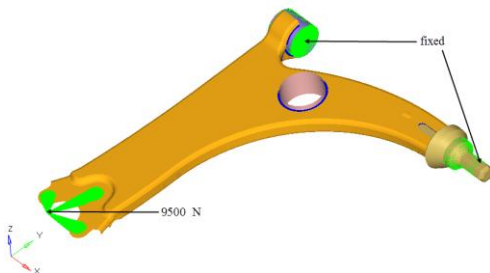


Figure 14. The schematic representation of Strength test

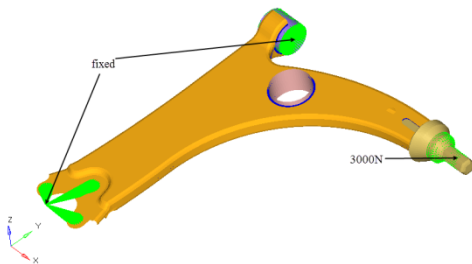


Figure 15. The schematic representation of Durability test

In order to further verify the reliability of lower control arm under the complete vehicle state, complete vehicle road reliability test is carried out according to design standards and specifications. The test roads are divided into expressway, twisted road, convex block road, long wave road, short wave road and washboard road. The test mileage is 50,000 km in total, and no abnormal vibration and cracking fault occur during the test. In conclusion, the entire finite element modeling, modal analysis, strength analysis and optimization design method have high accuracy and stability, which can provide reliable analysis methods and references for other similar structures.

7. Conclusion

1. The electric SUV lower control arm model is established by using finite element method on the Hypermesh software; the free modal analysis is carried out using Nastran software; the first and second order natural frequencies are 610.8 Hz and 693.5 Hz respectively. Free modal Test on lower control arm is conducted based on hammer method and LMS test. Lab platform, and the

relative error between the Test value and the analysis value is within a reasonable range.

2. On the basis of the lower control arm load extracted from the dynamics model of front suspension Adams/Car, the intensity analysis of the typical operating conditions is carried out to obtain that the maximum stresses in acceleration, turning and vertical conditions are 301.2 MPa, 98.7 MPa and 62.5 MPa, which are all lower than its permitted stress.
3. The multi-discipline and multi-objective optimization design are carried out on structure parameters of lower control arm using Isight platform to obtain the optimal value of its structural parameters. Namely: the thickness of lower control arm upper board is 3.6 mm, the thickness of lower board thickness is 3.2 mm, and the thickness of reinforced shaft tube is 3.5 mm. After optimization, the first and second order modal frequencies of lower control arm are 585.7 Hz and 661.2 Hz respectively, which meets the requirements of modal characteristics; the maximum stress of lower control arm is 346.4 MPa, and its strength safety coefficient meets the actual engineering requirements; the mass of lower control arm is successfully reduced by 16.7%, with a significant lightweighting effect.
4. The optimization scheme of lower control arm is analyzed using bench test and vehicle road test, which has successfully passed the test verification, so it has high accuracy and feasibility.

References

- [1] Fuchs, H.; Salmon, R. Lightweight MacPherson strut suspension front lower control arm design development. SAE 2011 World Congress and Exhibition 2011.
- [2] Yoo, S.H.; Doh, J.; Lim, J.H., et al. Topologically optimized shape of CFRP front lower control ARM. International Journal of Automotive Technology 2017, 18(4), 625-630.
- [3] Heo, S.J.; Kang, D.O., Lee, J.H., et al. Shape optimization of lower control arm considering multi-disciplinary constraint condition by using progress meta-model method. International Journal of Automotive Technology 2013, 14(3), 499-505.
- [4] Huang, H. Lightweight optimal design and fatigue performance analysis of control arm under the suspension. Changchun, China: Jilin University, Master's thesis, 2016.
- [5] Hou, K.; Sun, H.W. Static characteristics and modal analysis of carframe of a new semi-trailer. Mechanical Design and Manufacturing 2017, (8), 172-174.
- [6] Xu, G.Q. Optimal design of dimensions of front spline shaft for automobile drive shaft based on Isight. Chinese Science and Technology Paper 2017, 12(4), 408-411.
- [7] Soria, L.; Peeters, B.; Anthonis, J., et al. Operational modal analysis and the performance assessment of vehicle suspension systems. Shock and Vibration 2012, 19(5), 1099-1113.
- [8] Kronast, M., Theory and application of modal analysis in vehicle noise and vibration refinement. Vehicle Noise and Vibration Refinement 2010, 117-141.
- [9] Liu, J.B. NVH analysis and optimization research on body structure of a certain light truck based on FEA. Taiyuan, China: North University of China, Master's thesis, 2018.
- [10] Yin, H.J.; Liu, Y.; Wang, Y., et al. Modal analysis of a certain metal fuel tank and improvement of its partition structure. Machine Design 2017, 34(11), 94-97.
- [11] Huang, C.F.; Wang, P.; He, M.C., et al. Free vibration analysis of large composite truss structure section using hammer

- method. Journal of National University of Defense Technology 2018, 40(1), 37-41.
- [12] Bao, J.; Jing, J.P.; Zhou, H.W. Research on influence of bolt connection on combustion chamber structure mode of gas turbine. Noise and Vibration Control 2018, 38(5), 134-138.
- [13] Afefy, I.H.; Mohib, A.; El-kamash, A.M., et al. A new framework of reliability centered maintenance. Jordan Journal of Mechanical and Industrial Engineering 2019, 13(3), 175-190.
- [14] Gong, J. Acceleration sensor abnormality detection method for axle box of unmanned vehicle. Jordan Journal of Mechanical and Industrial Engineering 2020, 14(1), 149-158.
- [15] Chen, M. Design and optimization of car sub-frame. Hefei, China: Hefei University of Technology, 2010.
- [16] Zhou, J.C.; Yuan, J.; Liao, Y.H., et al. Optimization of Macphersan suspension based on D-optimal test design. Chinese Journal of Construction Machinery 2018, 16(5), 443-447.
- [17] Zhang, Z.F.; Chen, R.; Xu, Z.M., et al. Research on topology optimization of multi-objective vehicle suspension control arm. Journal of Mechanical Engineering 2017, 53(4), 114-121.
- [18] Li, M.; Liu, B.; Zhang, L. Optimization design of key structural parameters of high-speed train head type aerodynamic shape. Journal of Mechanical Engineering 2016, 52(20), 120-125.